



# Strength and engineering properties of cementless paste produced by GGBFS and MgO

Chao-Lung Hwang<sup>1</sup>, Duy-Hai Vo<sup>2</sup>, Khanh-Dung Tran Thi<sup>1</sup> and Mitiku Damtie Yehualaw<sup>1</sup>

<sup>1</sup>Department of Civil and Construction Engineering

National Taiwan University of Science and Technology, Taipei, Taiwan

<sup>2</sup>Faculty of Civil Engineering, University of Technology and Education,

The University of Danang, No. 48 Cao Thang street, Danang city, Vietnam

mikehwang@mail.ntust.edu.tw; duyhai88@gmail.com;

khanhdungtran412@gmail.com; mtkdmt2007@gmail.com

**Abstract.** This study aims to investigate engineering properties of cementless pastes which were produced by reactive magnesium oxide (MgO) and ground granulated blast furnace slag (GGBFS). The mixtures were designed in various levels of MgO at 2.5%, 5%, 7.5%, 10%, 15% and 20% of total binder weight. The slump flow test, compressive strength test, ultrasonic pulse velocity test (UPV) and thermal conductivity test were conducted to examine the engineering properties of the pastes until 28 curing days. The results indicate that the high proportion of MgO causes the decrease of flow-ability of fresh pastes. Increasing MgO content significantly promotes the hydration process and improves the compressive strength and hardened properties of pastes through the UPV and thermal conductivity testing results.

**Keywords:** cementless paste, compressive strength, engineering properties, thermal conductivity.

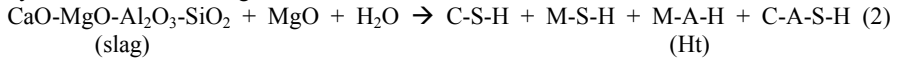
## 1 Introduction

The increase of cement demand to adapt the sharp improvement of construction industry has been generating a vast volume of CO<sub>2</sub> during the decarbonization in cement production process [1, 2]. Numerous studies have been carried out to research proper alternative construction materials. Alkali-activated materials namely alkali-activated slag and geo-polymers with the presence of sodium hydroxide (NaOH) and sodium silicate (Na<sub>2</sub>SiO<sub>3</sub>) are considered as the current attractive replacements. These materials have been proved to be eco-friendly and to satisfy the specification requirements such as high compressive strength in early stage, low permeability, good chemical resistance, and exceptional fire resistance [3, 4]. However, the residual alkali after reactions can contaminate surrounding environment [5, 6]. Therefore, substituting these solutions by an equivalently effective but less harmful substance is needed. Magnesium oxide (MgO), an

expansion agent, is potential to activate ground granulated blast-furnace slag (GGBFS) [1, 7] to produce alkali-activated slag (AAS). During the mixing process, MgO reacts with water to create an alkaline environment.



The alkaline environment breaks covalent bonds (Si-O-Si; Al-O-Si) in slag particles. The hydration reaction of MgO-GGBFS can be summarized as followed:



However, the current researches concerning this issue are still limited. So, this study attempts to use MgO as an activator for GGBFS in different contents: from 2.5% to 20% by weight of binder. Some fresh and hardened properties of the pastes were investigated by flow-ability tests, compressive strength tests, UPV, and thermal conductivity.

## 2 Materials and mix design

### 2.1 Materials

**Table 1.** Physical properties and chemical compositions of raw materials.

Items		GGBFS	MgO
Physical properties	Specific gravity	2.98	2.91
	Mean particle size ( $\mu\text{m}$ )	14.563	5.598
	Specific surface area ( $\text{m}^2/\text{g}$ )	1.44	2.12
Chemical composition (wt.%)	SiO <sub>2</sub>	33.39	8.34
	Al <sub>2</sub> O <sub>3</sub>	14.39	-
	Fe <sub>2</sub> O <sub>3</sub>	0.19	0.14
	CaO	41.08	0.42
	MgO	7.22	90.4
	SO <sub>3</sub>	0.11	0.75
	Basicity	1.88	-
	Sulfide sulfur	0.72	-

In this study, GGBFS and MgO were the source materials. Both materials were collected from a local company in Taiwan. Table 1. indicated the physical properties and chemical compositions of GGBFS and MgO. Fig. 1a and Fig. 1b respectively give information about particle size distributions (PSD) and XRD analysis of the raw materials.

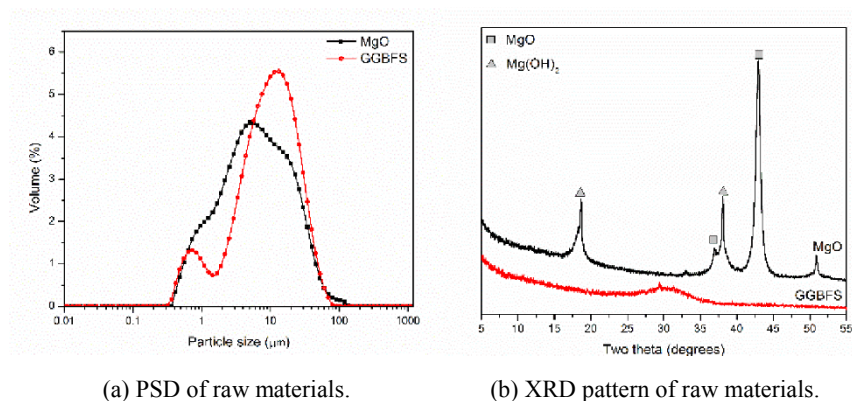


**Fig. 1.** Particle size distributions and XRD analysis of raw materials

## 2.2 Samples preparation

**Table 2.** Mix proportion of GGBFS-MgO cementless paste of 1000g powder.

Items	w/b	Slag	MgO	Water	Flow-ability (mm)
M2.5		975	25	350	230
M5		950	50	350	230
M7.5	0.35	925	75	350	230
M10		900	100	350	220
M15		850	150	350	200
M20		800	200	350	180

In this study, the mixtures were prepared with GGBFS and MgO. The MgO content was set at 2.5%, 5%, 7.5%, 10%, 15% and 20% of the total binder weight. The water-to-binder ratio was fixed at 0.35 for all of mixtures. Firstly, MgO was dissolved in water in 2 mins, and then GGBFS was added and mixed in 2 mins. Finally, the rest water was mixed in 3 mins to achieve a homogeneous fresh paste. After mixing, flow-ability of the paste was tested by flow table test. The 50x50x50mm cubic molds were prepared for compressive strength test while the cylinder 50x100mm samples were used for UPV test and thermal conductivity test. All of the samples were covered by a thin film to prevent water evaporation and were cured in ambient condition with  $50 \pm 5\%$  humidity and at  $25 \pm 2^\circ\text{C}$ . After 24 hours, the samples were demolded and cured in a water container at  $25 \pm 2^\circ\text{C}$  for compressive strength and UPV test, while other cylinder samples were cured in a chamber with  $50 \pm 5\%$  humidity and at  $25 \pm 2^\circ\text{C}$  for thermal conductivity analysis. The

compressive strength test, thermal conductivity and UPV complied to ASTM C109, ASTM C518 and C597, respectively.

### 3 Results and discussion

#### 3.1 Flow-ability

Table 2. presents the flow-ability values of GGBFS-MgO cementless pastes. It can be seen that the flow-ability was stable when the amount of GGBFS replaced by MgO steadily increased up to 7.5% and this figure gradually declined when the MgO content gained 10% and more. The decrease of workability was associated with the increase of MgO level. Compared to GGBFS particles, the specific surface area of MgO is much higher, resulting in the greater water absorption and thus, leading to the reduction of flow values [8].

#### 3.2 Compressive strength

The compressive strength of the pastes is illustrated in Fig. 2. As expected, the pastes gained more strength with curing time. Throughout 28 days, the pastes became denser and produced more strength due to the improvement of the amount of hydration products. Additionally, the more MgO content incorporating to the mixtures, the higher compressive strength the pastes will gain. Particularly, the compressive strength achieved the highest values in the mixture with 15% wt.% MgO content, considerably in the early ages. This phenomenon caused by the coexistence of C-S-H gel and hydrotalcite (Ht) formed in the hydration processes [7-9]. However, as the MgO content exceeded 15%, the compressive strength of the pastes began dropping. When MgO/GGBFS ratio increased, the amount of aluminosilicate content declined, which partly mitigated the volume of C-S-H gel. Furthermore, the rise of Ht, which is believed to be more voluminous than C-S-H [7], properly led to the volume instability of the pastes structure [8].

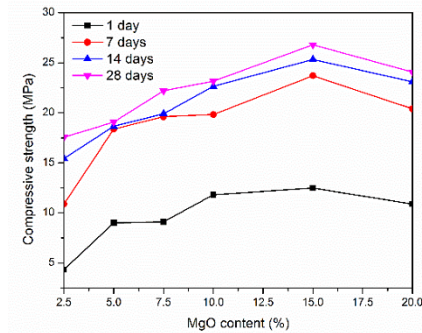


**Fig.2.** Effect of MgO content on compressive strength development of cementless pastes.

### 3.3 UPV results

Fig. 3 indicates the development of UPV values with curing up to the 28<sup>th</sup> day. The improvement of UPV values likewise was similar to that of the compressive strength [10]. The UPV results improved with increasing MgO levels. The figures were the highest in the paste with 15 wt.% MgO of total binder and then going down as the MgO content was over 15%. The explanation for these phenomena was alike to those of the compressive strength as discussed above. C-S-H and Ht filled pores in the hardened pastes and formed denser pastes, resulting in the higher values of UPV during the curing time. However, more than 15% MgO content reduced the UPV values. The growth of MgO mass was equivalent to the reduction of GGBFS in the mixture. That led to the corresponding decrease of aluminosilicate and subsequent hydration products [8].

### 3.4 Thermal conductivity

Fig. 4 informs thermal conductivity data of the pastes under the curing period. Thermal conductivity evaluated the heat conductivity capability of the pastes [11]. The previous studies revealed several factors on thermal conductivity such as type of materials, proportioning, moisture content, density, porosity, and curing condition. The thermal conductivity recorded on 28<sup>th</sup> day was far lower than that on 7<sup>th</sup> day. The thermal conductivity value declined due to the loss of water by evaporation and hydration process. Specifically, on the 28<sup>th</sup> day, the thermal conductivity was the lowest in 2.5%-MgO mixture. The thermal conductivity rose with increasing MgO content, which can be attributed to the highly conductive nature of MgO [12].

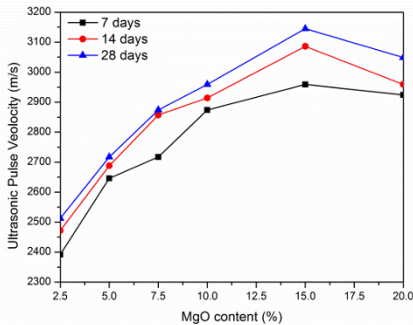


**Fig.3.** Effect of MgO content on UPV values of cementless pastes.

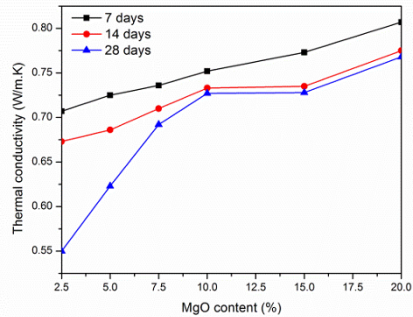


**Fig.4.** Effect of MgO content on thermal conductivity of cementless pastes.

## 4 Conclusion

Based on the experimental works of the present study, the following conclusions can be drawn:

1. Using the high amount of MgO (over 10%) in the binder causes negative effects on workability of the cementless pastes.
2. The compressive strength and UPV results of the paste samples significantly improve with increasing MgO contents. The optimal mixture is the incorporation of 15% MgO and 85% GGBFS. The higher proportion of MgO reduces the strength and UPV value in comparison with the optimal mixture.
3. Thermal conductivity of the cementless pastes gradually increases with the growth of MgO content.

## References

- [1] K. Gu, F. Jin, A. Al-Tabbaa, B. Shi, J. Liu, Mechanical and hydration properties of ground granulated blastfurnace slag pastes activated with MgO–CaO mixtures, *Construction and Building Materials* 69 (2014) 101-108.
- [2] S.A. Miller, V.M. John, S.A. Pacca, A. Horvath, Carbon dioxide reduction potential in the global cement industry by 2050, *Cement and Concrete Research* 114 (2018) 115-124.
- [3] C. Carreño-Gallardo, A. Tejada-Ochoa, O.I. Perez-Ordóñez, J.E. Ledezma-Sillas, D. Lardizabal-Gutierrez, C. Prieto-Gomez, J.A. Valenzuela-Grado, F.C. Robles Hernandez, J.M. Herrera-Ramirez, In the CO<sub>2</sub> emission remediation by means of alternative geopolymers as substitutes for cements, *Journal of Environmental Chemical Engineering* 6(4) (2018) 4878-4884.
- [4] J.L. Provis, Alkali-activated materials, *Cement and Concrete Research* 114 (2018) 40-48.
- [5] S. Paulose, P. Reddy, J. Kv, Swell Potential Studies on Soils Contaminated with NaOH Solutions, 2014.
- [6] R.V.P. Chavali, S.K. Vindula, H.P.R. P, A. Babu, R.J. Pillai, Swelling behavior of kaolinitic clays contaminated with alkali solutions: A micro-level study, *Applied Clay Science* 135 (2017) 575-582.
- [7] F. Jin, K. Gu, A. Al-Tabbaa, Strength and hydration properties of reactive MgO-activated ground granulated blastfurnace slag paste, *Cement and Concrete Composites* 57 (2015) 8-16.
- [8] C.-L. Hwang, D.-H. Vo, V.-A. Tran, M.D. Yehualaw, Effect of high MgO content on the performance of alkali-activated fine slag under water and air curing conditions, *Construction and Building Materials* 186 (2018) 503-513.
- [9] S.A. Bernal, R. San Nicolas, R.J. Myers, R. Mejía de Gutiérrez, F. Puertas, J.S.J. van Deventer, J.L. Provis, MgO content of slag controls phase evolution and structural changes induced by accelerated carbonation in alkali-activated binders, *Cement and Concrete Research* 57 (2014) 33-43.
- [10] T. Yılmaz, B. Ercikdi, K. Karaman, G. Külekçi, Assessment of strength properties of cemented paste backfill by ultrasonic pulse velocity test, *Ultrasonics* 54(5) (2014) 1386-1394.
- [11] I. Asadi, P. Shafiqh, Z.F.B. Abu Hassan, N.B. Mahyuddin, Thermal conductivity of concrete – A review, *Journal of Building Engineering* 20 (2018) 81-93.
- [12] H. Yuan, Y. Shi, Z. Xu, C. Lu, Y. Ni, X. Lan, Effect of nano-MgO on thermal and mechanical properties of aluminate cement composite thermal energy storage materials, *Ceramics International* 40(3) (2014) 4811-4817.